[30] K. Greish, J. Fang, T. Inutsuka, A. Nagamitsu, H. Maeda, Macromolecular therapeutics: advantages and prospects with special emphasis on solid tumour targeting, Clin. Pharmacokinet. 42 (2003) 1089–1105.
[31] T. Nakanishi, S. Fukushima, K. Okamoto, M. Suzuki, Y. Matsumura, M. Yokoyama, T. Okano, Y. Sakurai, K. Kataoka, Development of the polymer micelle carrier system for doxorubicin, J. Control. Release 74 (2001) 295–302.
[32] H. Maeda, J. Wu, T. Sawa, Y. Matsumura, K. Hori, Tumor vascular permeability and the EPR effect in macromolecular therapeutics: a review, J. Control. Release 65 (2000) 271–284.
[33] J.W. Park, Liposome-based drug delivery in breast cancer treatment, Breast Cancer Res. 4 (2002) 95–99.
[34] A. Di Paolo, Liposomal anticancer therapy: pharmacokinetic and clinical aspects, J. Chemother. 4 (2004) 90–93.
[35] K. Yun, E. Kobatake, T. Haruyama, M.L. Laukkanen, K. Keinanen, M. Aizawa, Use of a quartz crystal microbalance to monitor immunoliposome-antigen interaction, Anal. Chem. 70 (1998) 260–264.
[36] T. Terada, M. Nishikawa, F. Yamashita, M. Hashida, Influence of cholesterol composition on the association of serum mannan-binding proteins with mannosylated liposomes, Biol. Pharm. Bull. 29 (2006) 613–618.
[37] S. Lin, C.C. Lu, H.F. Chien, S.M. Hsu, An on-line quantitative immunoassay system based on a quartz crystal microbalance, J. Immunol. Methods 239 (2000) 121–124.
[38] T. Terada, M. Nishikawa, F. Yamashita, M. Hashida, Analysis of the molecular interaction between mannosylated proteins and serum mannan-binding lectins, Int. J. Pharm. 316 (2006) 117–123.
[39] O. Ishida, K. Maruyama, K. Sasaki, M. Iwatsuru, Size-dependent extravasation and interstitial localization of polyethyleneglycol liposomes in solid tumor-bearing mice, Int. J. Pharm. 190 (1999) 49–56.
[40] G.J. Charrois, T.M. Allen, Rate of biodistribution of STEALTH liposomes to tumor and skin: influence of liposome diameter and implications for toxicity and therapeutic activity, Biochim. Biophys. Acta 1609 (2003) 102–108.
[41] P. Sapra, T.M. Allen, Ligand-targeted liposomal anticancer drugs, Prog. Lipid Res. 42 (2003) 439–462.
[42] K. Maruyama, T. Takizawa, T. Yuda, S.J. Kennel, L. Huang, M. Iwatsuru, Targetability of novel immunoliposomes modified with amphipathic poly (ethylene glycol)s conjugated at their distal terminals to monoclonal antibodies, Biochim. Biophys. Acta 1234 (1995) 74–80.
[43] S.M. Plum, J.W. Holaday, A. Ruiz, J.W. Madsen, W.E. Fogler, A.H. Fortier, Administration of a liposomal FGF-2 peptide vaccine leads to abrogation of FGF-2-mediated angiogenesis and tumor development, Vaccine 19 (2000) 1294–1303.

Available online at www.sciencedirect.com
ScienceDirect
Journal of Controlled Release 125 (2008) 121–130
journal of controlled release
www.elsevier.com/locate/jconrel

Efficient targeting to alveolar macrophages by intratracheal administration of mannosylated liposomes in rats

Wassana Wijagkanalan [a], Shigeru Kawakami [a], Mitsuko Takenaga [b], Rie Igarashi [b], Fumiyoshi Yamashita [a], Mitsuru Hashida [a,*]

[a] Department of Drug Delivery Research, Graduate School of Pharmaceutical Sciences, Kyoto University, Sakyo-ku, Kyoto, 606-8501, Japan
[b] Institute of Medical Science, St. Marianna University School of Medicine, Miyamae-ku, Kawasaki, 216-8512, Japan

Received 23 July 2007; accepted 14 October 2007
Available online 22 October 2007

Abstract

The success of targeting systems to alveolar macrophages critically depends on internalization into these cells for pharmacological intervention. Direct respiratory delivery via inhalation of mannose modified liposomal carriers to alveolar macrophages is of great interest. To evaluate the targeting efficiency to alveolar macrophages by intratracheal administration of mannosylated liposomes (Man-liposomes), Man-liposomes with various ratio of mannosylated cholesterol derivatives, cholesten-5-yloxy-*N*-(4-((1-imino-2-D-thiomannosylethyl)amino)alkyl)formamide (Man-C4-Chol) as mannose receptor ligand were investigated with regard to their *in vitro* uptake in primary cultured alveolar macrophages and *in vivo* intratracheal administration in rats. The *in vitro* uptake of Man-liposomes took place in a concentration-dependent manner. The internalization of Man-liposomes with 7.5% (Man-7.5-liposomes) and 5.0% (Man-5.0-liposomes) Man-C4-Chol was considerably higher than that of Man-liposomes with 2.5% of Man-C4-Chol (Man-2.5-liposomes) and Bare-liposomes and significantly inhibited by an excess of mannan, suggesting mannose receptor-mediated endocytosis. After intratracheal administration of Man-7.5 and Man-5.0-liposomes in rats, a significantly high internalization and selective targeting to alveolar macrophages was observed. The enhanced cellular uptake in alveolar macrophages related to the mannose density of Man-liposomes was also confirmed both *in vitro* and *in vivo* confocal microscopy studies. These results demonstrate the efficient targeting to alveolar macrophages by the intratracheally administered Man-liposomes via mannose receptor-mediated endocytosis.

Keywords: Drug delivery; Inhalation; Macrophage; Mannose receptor; Targeting

1. Introduction

Today, pulmonary conditions including inflammation and infectious diseases are critical health problem. Alveolar macrophages are key effector cells in the first-line host defense [18] and lung homeostasis [27]. Pulmonary delivery via inhalation, non-invasive administration for local [7] and systemic effects [3], offers optimal bioavailability by reducing first-pass metabolism in the liver, reducing side effects, and improving patient compliance. Therefore, much effort has been directed toward the development of cell-selective targeting systems to macrophages using a variety of carriers to improve therapeutic efficiency and minimize side effects [13,26,30].

Liposomes have been considered as a potential drug and/or gene carrier due to enabling the loading capacity for a variety of compounds, allowing chemical modification for a wide range of applications, minimizing the systemic toxicity of the incorporated drugs and improving their stability [9,11,12,21,30]. Since mannose receptors, a 175 kDa transmembrane protein of the C-type lectin family, are exclusively expressed on the surface of alveolar macrophages that can recognize mannose terminal molecules with high affinity [14], mannosylation of liposomes is an attractive approach for cell-selective targeting to alveolar macrophages. We have previously reported macrophage-selective targeting by mannosylated liposomes (Man-liposomes) composed of novel mannosylated cholesterol derivatives,

* Corresponding author. Tel.: +81 75 753 4525; fax: +81 75 753 4575.
E-mail address: hashidam@pharm.kyoto-u.ac.jp (M. Hashida).

0168-3659/$ - see front matter © 2007 Elsevier B.V. All rights reserved.
doi:10.1016/j.jconrel.2007.10.011

cholesten-5-yloxy-*N*-(4-((1-imino-2-D-thiomannosylethyl) amino)butyl)formamide (Man-C4-Chol), as a ligand for mannose receptors [12]. After intravenous administration to mice, Man-liposomes are rapidly and preferentially delivered to the hepatic non-parenchymal cells including Kupffer cells, via mannose receptor-mediated uptake [11,12,21]. However, targeting efficiency of Man-liposomes to alveolar macrophages by intratracheal administration could not be predicted. These observations prompted us to investigate whether Man-liposomes has a great potential as alveolar macrophage-selective targeting carriers administered via inhalation.

It has been reported that the efficient uptake of carrier systems is affected by the ligand density [34] and physiological environment [1,28,29]. A pulmonary surfactant (PS) composed of phospholipids (90%) and proteins (10%) is secreted as multilamellar assemblies from alveolar epithelial type II cells and is removed by alveolar epithelial type II cells and alveolar macrophages in order to obtain homeostasis [22]. PS, especially surfactant proteins, has been demonstrated to intercalate in the liposomal membrane [31] leading to leakage of encapsulated substances [1,29], to alter the uptake of liposomes by alveolar cells [23] and reduce the efficiency of gene transfer [28].

The aim of this study was to evaluate the targeting efficiency of Man-liposomes to alveolar macrophages by direct pulmonary delivery. Man-liposomes composed of 1,2-distearoyl-*sn*-glycero-3-phosphocholine (DSPC), Cholesterol (Chol) and Man-C4-Chol with different molar ratios were characterized in a series of *in vitro* and *in vivo* studies. *In vitro* uptake of Man-liposomes was investigated in primary cultured rat alveolar macrophages. *In vivo* targeting of Man-liposomes was also studied after intratracheal administration in rats.

2. Materials and methods

2.1. Materials

DSPC and sulforhodamine B were purchased from Sigma-Aldrich, Co. (St. Louis, MO, USA). *N*-(fluorescein-5-thiocarbamoyl)-1,2-dihexadecanoyl-*sn*-glycero-3-phosphoethanolamine, triethylammonium salt (fluorescein DHPE, F-DHPE) was obtained from Molecular Probes, Inc. (Eugene, OR, USA). Rhodamine Concanavalin A conjugate (RhoConA), maclura pomifera agglutinin (MPA) biotinylated lectins and Texas Red steptavidin were provided by Vector Laboratories, Inc. (Burlingame, CA, USA). *Griffonia simplicifolia* (GS)-I lectin was obtained from EY Laboratories, Inc. (San Mateo, CA, USA). All other chemicals used were of the highest purity available.

2.2. Preparation of liposomes

Man-C4-Chol was synthesized by the method described previously [12,15]. Fluorescent-labeled liposomes consisting of DSPC, Chol, F-DHPE and Man-C4-Chol at various molar ratios was prepared; Bare-liposomes (60:35:5:0), Man-2.5-liposomes (60:32.5:5:2.5), Man-5.0-liposomes (60:30:5:5) and Man-7.5-liposomes (60:27.5:5:7.5). The lipid mixtures were dissolved in chloroform and then evaporated. The dried film was vacuum-desiccated, and resuspended in pH 7.4 PBS. For the stability study of liposomes in PS, carboxyfluorescein (CF)-liposomes were prepared by hydrating a lipid film containing DSPC, Chol and Man-C4-Chol, with 60 mM CF solution. The resulting liposomes were sonicated and extruded through 200- and 100-nm polycarbonate membrane filters using an extruder device preheated to 60 °C. Free CF was removed from CF-liposomes by gel chromatography using a Sephadex® G-25 M; PD-10 column (GE Healthcare, Uppsala, Sweden). The particle sizes of the liposomes were determined using a Zetasizer Nano ZS instrument (Malvern Instruments, Ltd., Worcestershire, UK). The concentration of the liposomes was measured using a Cholesterol E-test kit (Wako Pure Chemical Industries, Ltd., Osaka, Japan).

2.3. Animals

Eight-week-old male wistar rats (250–300 g) were obtained from the Shizuoka Agriculture Cooperative Association for Laboratory Animals (Shizuoka, Japan). All animal experiments were carried out in accordance with the Principles of Laboratory Animal Care as adopted and propagated by the US National Institutes of Health and the Guidelines for Animal Experiments of Kyoto University.

2.4. Isolation of alveolar macrophages and alveolar epithelial type II cells

Rats were euthanized and the thorax was opened, then the lung blood circulation was removed with sterile balanced salt solution (BSSA) (137 mM NaCl, 5 mM KCl, 0.7 mM Na_2HPO_4, 10 mM HEPES, and 5.5 mM glucose), pH 7.4 via the pulmonary artery. The lung was removed from the thoracic cavity *en bloc* and lavaged with a 10 mL of EDTA-BSSA for a total five washes. The bronchoalveolar lavage fluid (BALF) were pooled for each animal and centrifuged at 200 $\times g$ for 10 min at 4 °C. The alveolar macrophages were obtained after washing once with ice-cold PBS. Alveolar epithelial type II cells were further isolated using the method modified from Mason et al. [17] and our previous report [10]. The alveolar epithelial type II-enriched cells were incubated with 16 μg/mL GS-I lectin to remove contaminating alveolar macrophages, as described by Simon et al. [25]. The alveolar epithelial type II cells were obtained after washing with ice-cold PBS. The cell viability was greater than 99% measured using the trypan blue exclusion method. Cell differentiation was determined by the modified-Giemsa stain method (Diff-Quik®, Sysmex, Japan). The average yield of alveolar macrophages and alveolar epithelial type II cells was 3.18×10^6 and 11.54×10^6 cells/rat, respectively.

2.5. Isolation of native pulmonary surfactant (PS)

Rat lung surfactant was isolated by density gradient centrifugation of blood-free BALF using the method described by Bernhard et al. [2]. The surfactant concentration was measured

using the phosphorous assay method using a PL-C kit (Wako Pure Chemical Industries, Ltd., Osaka, Japan).

2.6. In vitro uptake study

Isolated alveolar macrophages were cultured in RPMI 1640 supplemented with 10% heat-inactivated fetal bovine serum at a density of 2.1×10^5 cells/cm^2 for 12 h before uptake experiment. Alveolar macrophages were washed with Hank's Balance Salt Solution (HBSS), and then incubated with fluorescent-labeled liposomes at a lipid concentration range of 10–200 μM for the indicated time (0.5–2 h). For the inhibition study, alveolar macrophages were incubated for 2 h with a mixture of liposomes (50 μM) and inhibitors (1 mg/mL mannan or bare-liposomes) or pre-incubated with 1 mM of iodoacetate; most effective endocytotic inhibitor, for 30 min prior to liposomes [6]. To investigate the effect of PS in the uptake study, CF-liposomes were incubated with 0.1 mg/mL lipid concentration of native PS [1,28]. For the internalization study, the cells were washed five times with ice-cold PBS containing 20 mM EDTA to remove the liposomes bound to the cell surface [19]. Finally, the cell pellet was resuspended in ice-cold PBS. The cell-associated fluorescence in 10000 cells was measured using a FACSCalibur flow cytometer (Becton Dickinson, NJ, USA). Cells from the non-treatment group were used to determine the autofluorescence.

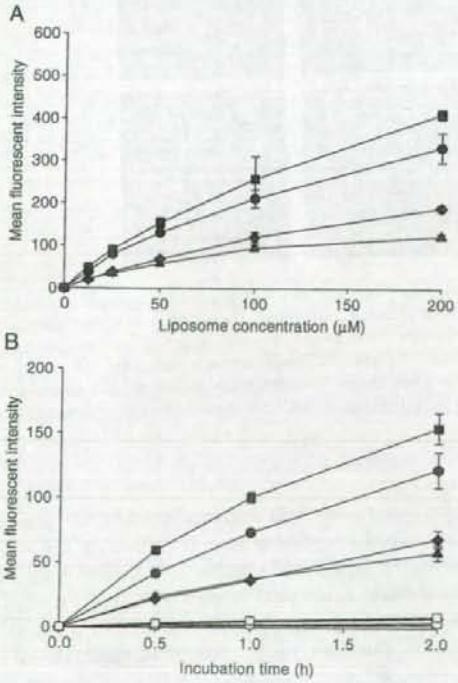

Fig. 1. (A) Dose-dependent *in vitro* uptake of Bare- (◆), Man-2.5- (▲), Man-5.0- (●), and Man-7.5-liposomes (■). Isolated alveolar macrophages were incubated with different lipid concentrations of liposomes at 37 °C for 2 h. (B) The *in vitro* uptake time-course of 50 μM liposomes described above at 4 (opened symbols) or 37 °C (filled symbols) for a given incubation time. Results are expressed the mean ± S.D. of three experiments.

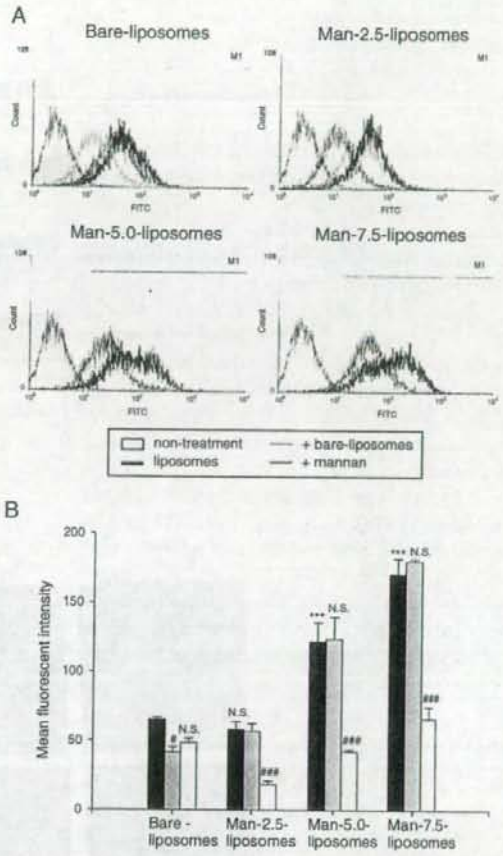

Fig. 2. The *in vitro* uptake of 50 μM liposomes by isolated alveolar macrophages. Isolated alveolar macrophages were incubated with each type of liposomes alone as control (filled column) or in the presence of 1 mg/mL bare-liposomes (shaded column) or 1 mg/mL mannan (opened column). The histogram (A) and mean fluorescence (B) of liposomes associated with the cells was measured following a 2 h-incubation at 37 °C. Each value represents the mean ± S.D. of three experiments. Statistically significant differences (***$P<0.001$) from a control of Bare-liposomes, (#$P<0.05$; ###$P<0.001$) from a control for each group. N.S., not significant.

2.7. Stability of liposomes in pulmonary surfactant (PS)

Two micromolar of CF-liposomes were incubated with 0.1 mg/mL PS at 37 °C. At the indicated times, the fluorescence (F_t) was determined at a wavelength of 485/535 nm compared with the fluorescence at time zero (F_0) and the total fluorescence determined using 0.1% Triton X-100 (F_T). The CF release was calculated using the following equation:

$$\%\ \text{CF released} = \frac{(F_t - F_0)}{(F_T - F_0)} \times 100.$$

2.8. In vivo uptake study after intratracheal instillation

Fluorescent-labeled liposomes with a lipid concentration range 0.5–5 mg/kg were intratracheally instilled into the rat lungs using a Microsprayer® (PennCentury, Philadelphia, PA,

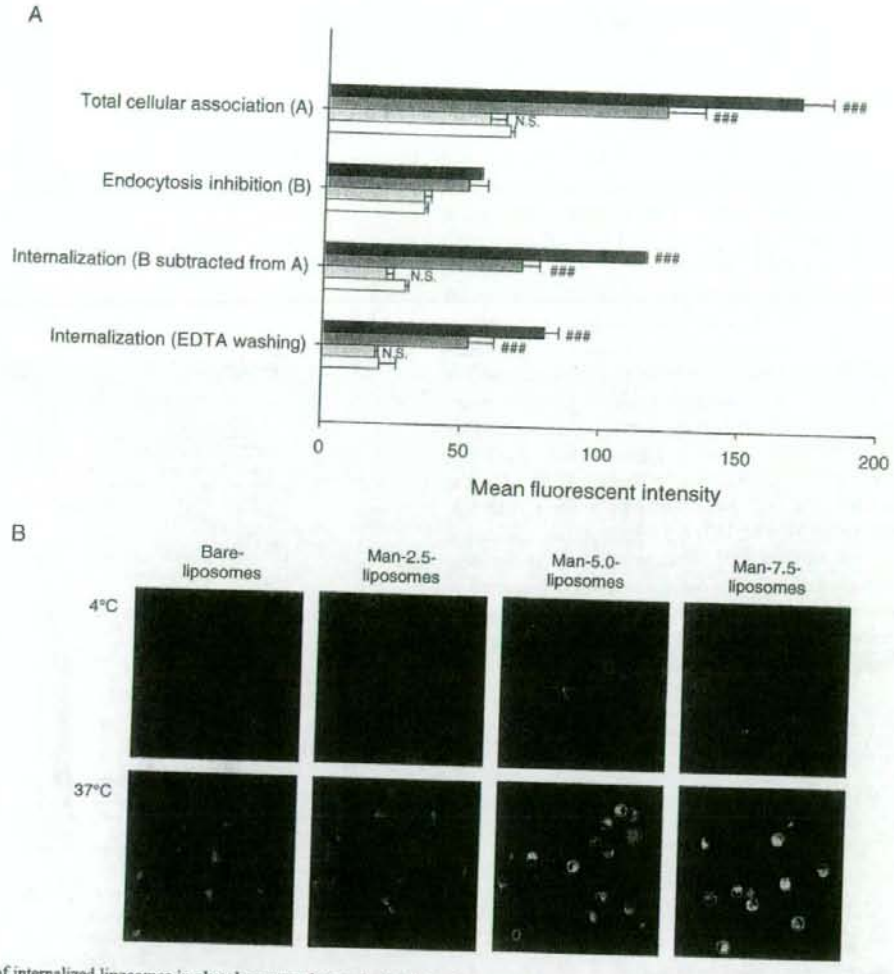

Fig. 3. (A) Amount of internalized liposomes in alveolar macrophages. Isolated alveolar macrophages were incubated with 50 μM of Bare- (white), Man-2.5- (light grey), Man-5.0- (dark grey), or Man-7.5- (black) liposomes under various condition as described in Materials and methods. The difference in mean cellular associated fluorescence between iodoacetate and ice-cold PBS treatment was regarded as the mean fluorescence of internalized liposomes in alveolar macrophages. Each value represents the mean ± S.D. of three experiments. Statistically significant differences (###$P<0.001$) compared with Bare-liposomes in each group, N.S., not significant. (B) *In vitro* confocal microscopy images of binding and internalization of fluorescent-labeled liposomes by alveolar macrophages. Isolated alveolar macrophages were incubated with 50 μM liposomes at 4 or 37 °C for 2 h. Liposomes and plasma membrane of alveolar macrophages were labeled with F-DHPE in green and RhoConA in red, respectively. The images are typical of at least three independent experiments.

USA). For the inhibition study, mannan at a dose 5 mg/kg was injected just before the administration of liposomes (3 mg/kg). Two hour after administration, alveolar macrophages and alveolar epithelial type II cells were isolated. The cell-associated fluorescence in 50,000 cells was measured as described above.

2.9. Confocal microscopy study

For the *in vitro* confocal microscopy study, 50 μM of fluorescent-labeled liposomes was incubated in 12-h pre-cultured alveolar macrophages at 4 or 37 °C for 2 h. For plasma membrane staining, fixed cells were incubated with 20 μg/mL RhoConA at room temperature for 5 min [34].

For the *in vivo* confocal microscopy study, the pulmonary tissue and alveolar epithelial type II cells were stained with sulforhodamine B and MPA lectin at 2 h after intratracheal administration of fluorescent-labeled liposomes, respectively [16]. In the tissue staining, the lung was initially perfused with 37 °C PBS containing 0.1% sulforhodamine B, pH 7.4, subsequently; the lung was fixed with fixative solution (0.6% formaldehyde-0.9% glutaraldehyde solution in 75 mM cacodylate buffer, pH 7.4) containing 0.1% sulforhodamine B. The fresh lung slices (500 μM in thickness) were then placed in a sample holder and a coverslip glass was applied. In the staining of alveolar epithelial type II cells, the lung was washed with HBSS after a 2 h-administration to remove alveolar

macrophages, and then incubated with 50 μg/mL MPA biotinylated lectin, a marker of alveolar epithelial type II cells. After a 1 h-incubation, the lung was incubated with 20 μg/mL Texas Red steptavidin for 1 h. The lung samples were sliced as described above after washing with HBSS. The *in vitro* and *in vivo* samples were examined using a MRC-1024 confocal laser microscope (Bio-Rad Laboratories Inc., Hercules, CA, USA). The objective specification was 60× oil immersion.

2.10. Statistical analysis

Statistical analysis was performed using ANOVA and the Turkey-Kramer test for multiple comparisons between groups. $P<0.05$ was considered to be indicative of statistical significance.

3. Results

3.1. Particle size of liposomes and in vitro uptake study

Among the various ratios of Man-C4-Chol containing liposomes, the mean particle size and zeta potential of liposomes ranged 90–125 nm with 0.14–0.35 polydispersity index and −9 to 15 mV, respectively.

To characterize the *in vitro* uptake of fluorescent-labeled Man-liposomes in alveolar macrophages, the cells were subjected to various conditions involving different doses, temperatures and incubation times. The uptake of Man-7.5- and Man-5.0-liposomes was markedly higher than that of Man-2.5- and Bare-liposomes and was dose-dependent (Fig. 1A). Fig. 1B shows the increased uptake of Man-7.5- and Man-5.0-liposomes over the incubation time to reach a plateau at 37 °C suggesting a time-dependent uptake mechanism; whereas, the uptake of all liposomes was retarded at 4 °C.

3.2. Uptake inhibition study

In order to investigate the uptake mechanism of Man-liposomes via mannose receptors in alveolar macrophages, liposomes were competitively taken up by alveolar macrophages with an excess of mannan, a known ligand for mannose receptors, or unlabeled bare-liposomes (Fig. 2). The uptake in term of the mean fluorescence of Man-7.5- and Man-5.0-liposomes was significantly higher than that of Man-2.5- and Bare-liposomes, which were comparable ($P<0.001$). In addition, the uptake of Man-liposomes was considerably inhibited in the presence of 1 mg/mL mannan ($P<0.001$), conversely, that of Bare-liposomes was significantly suppressed only by co-incubation with unlabeled bare-liposomes ($P<0.05$).

3.3. Internalization study

Since the internalization of carriers is important for the success of delivery systems, the internalization of Man-liposomes in alveolar macrophages triggered by mannose moieties was studied. To determine the amount of surface bound and internalized Man-liposomes in alveolar macrophages, cells were pre-incubated with 1 mM iodoacetate and washed with 20 mM EDTA in PBS, respectively (Fig. 3A). The internalization of Man-7.5- and Man-5.0-liposomes was significantly greater than that of Man-2.5- and Bare-liposomes ($P<0.001$). The pattern of internalization of liposomes obtained from these different methods was identical.

Fig. 3B shows confocal microscopy images of the cellular association of liposomes after a 2 h-incubation at 4 (binding) and 37 °C (internalization). These confocal microscopy images revealed a temperature-dependent internalization of liposomes. In addition, the internalization of Man-liposomes was increased with regard to the Man-C4-Chol content in a manner similar to that found in the *in vitro* uptake experiments.

3.4. In vivo uptake after intratracheal instillation

To evaluate the *in vivo* uptake characteristics of Man-liposomes, rats were intratracheally administered liposomes at a concentration of 0.5–5 mg/kg and alveolar macrophages were

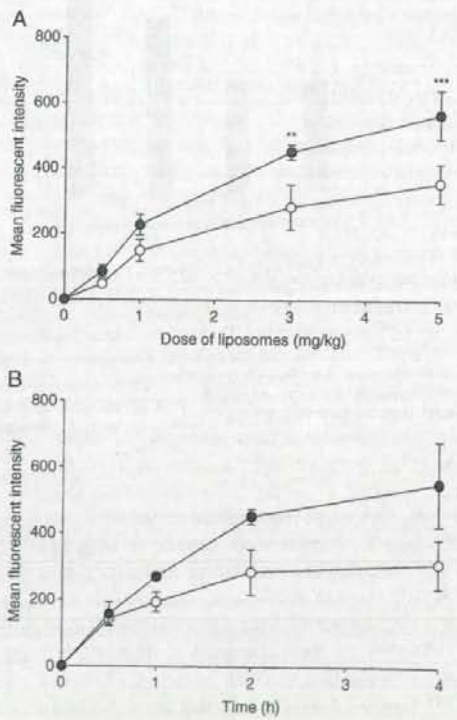

Fig. 4. (A) Dose-dependent uptake of Bare- (○) and Man-5.0- (●) liposomes *in vivo*. Two hours after intratracheal instillation of fluorescent-labeled liposomes in rats, alveolar macrophages were isolated and subjected to flow cytometry analysis. (B) The *in vivo* uptake time-course of Bare- (○) and Man-5.0- (●) liposomes. Rats received intratracheal administrations of fluorescent-labeled liposomes at 3 mg/kg. At the indicated times, alveolar macrophages were isolated and subjected to flow cytometry analysis. Each value represents the mean±S.D. of three experiments. Statistically significant differences (**$P<0.01$; ***$P<0.001$) compared with Bare-liposomes, N.S., not significant.

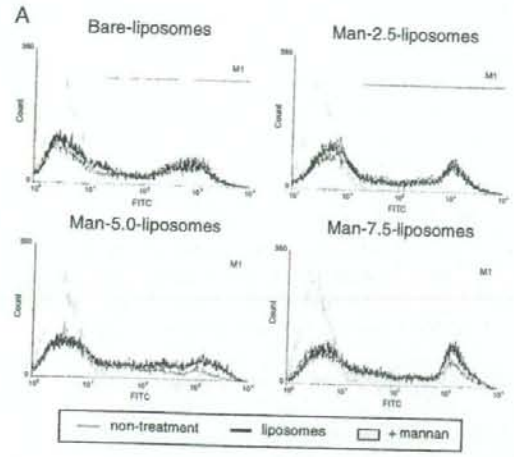

Fig. 5. The *in vivo* uptake of fluorescent-labeled liposomes after intratracheal instillation in rats. Rats were given each type of liposomes alone (filled column) at 3 mg/kg or pre-dosing with 5 mg/kg mannan (opened column); 2 h later, alveolar macrophages were isolated. The histogram (A) and mean fluorescence (B) of liposomes associated with the cells was measured by flow cytometry. Each value represents the mean±S.D. of three experiments. Statistically significant differences (*$P<0.05$; ***$P<0.001$) compared with a control of Bare-liposomes, (###$P<0.001$) from a control of each group. N.S., not significant.

isolated at various pre-determined times. The cell-associated fluorescence of alveolar macrophages in both Man-5.0- and Bare-liposomes showed a dose-dependent increase with a time-dependent maximum reaching a plateau after 2 h-incubation; however, the uptake of Man-5.0-liposomes was significantly higher than that of Bare-liposomes at dose 3 ($P<0.01$) and 5 ($P<0.001$) mg/kg (Fig. 4A–B).

To examine the *in vivo* uptake mechanism of Man-liposomes in a mannose receptor-mediated manner, rats were pre-administered with 5 mg/kg mannan prior to liposomes. Fig. 5 shows the significantly high association with alveolar macrophages of Man-7.5- ($P<0.001$) and Man-5.0-liposomes ($P<0.05$); and conversely, the comparable association of Man-2.5- and Bare-liposomes. After pre-treatment with mannan, the uptake of Man-7.5-and Man-5.0-liposomes was markedly hindered ($P<0.001$) but there was no significant difference in the uptake of Man-2.5- and Bare-liposomes.

3.5. Intrapulmonary localization after intratracheal instillation

To verify the cell-selective targeting ability of Man-liposomes, the pulmonary cells including alveolar macrophages and alveolar epithelial type II cells were isolated after a 2 h-intratracheal administration. Although all liposomes were preferentially associated with alveolar macrophages, Man-7.5- and Man-5.0-liposomes showed extensive association with alveolar macrophages, rather than alveolar epithelial type II cells, with a high uptake ratio compared with Man-2.5- and Bare-liposomes (Fig. 6). Furthermore, the number of alveolar macrophages (gated cells) involved in the uptake of Man-7.5 and Man-5.0-liposomes were 59 and 51%, respectively, which was around 2-times higher than that of Man-2.5 and Bare-liposomes (35%).

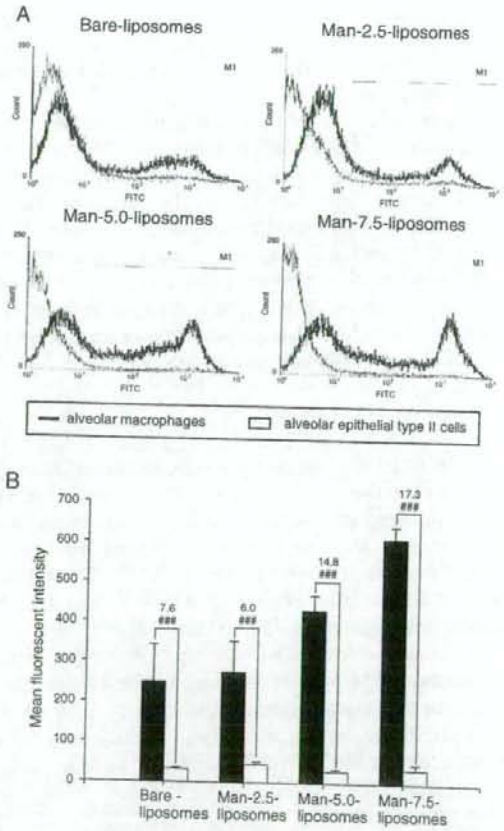

Fig. 6. Intrapulmonary localization of fluorescent-labeled liposomes after intratracheal administration in rats. Two hours after administration of liposomes at 3 mg/kg, alveolar macrophages (black) and alveolar epithelial type II cells (white) were isolated. The histogram (A) and mean fluorescent intensity (B) in both cell types were measured by flow cytometry. The uptake ratio by alveolar macrophages to alveolar epithelial type II cells was calculated. Each value represents the mean±S.D. of three experiments. Statistically significant differences (###$P<0.001$) in each group. N.S., not significant.

3.6. In vivo confocal microscopy study

These confocal microscopy images show the pulmonary disposition of fluorescent-labeled liposomes (green) in pulmonary tissue (red) after a 2 h-intratracheal instillation (Fig. 7A). Both liposomes homogeneously distributed in the lung alveoli and accumulated in large-sized particular cells located in the air space which are assumed to be alveolar macrophages (arrow); however, Man-5.0-liposomes exhibited a higher uptake than Bare-liposomes. To evaluate the cell-selective uptake of Man-liposomes, alveolar epithelial type II cells were stained with MPA-Texas red (Fig. 7B). Man-5.0- and Bare-liposomes were scarcely taken up by alveolar epithelial type II cells (upper panel). On the contrary, the accumulation of Man-5.0-liposomes was obviously greater than that of Bare-liposomes in isolated alveolar macrophages (lower panel).

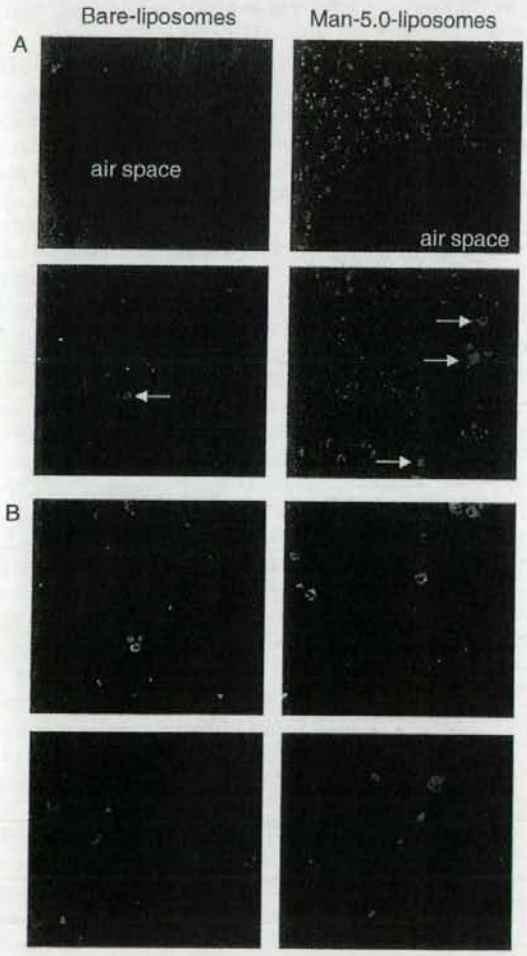

Fig. 7. *In vivo* confocal microscopy images of fluorescent-labeled liposomes (green) at 2 h following intratracheal administration. (A) Localization of liposomes in bronchi (upper panel) and alveoli (lower panel). After 2 h, the rat lung tissue was stained in red with sulforhodamine B. (B) Accumulation of liposomes in alveolar epithelial type II cells (upper panel) and alveolar macrophages (lower panel). After 2 h, alveolar macrophages were isolated and then alveolar epithelial type II cells were stained in red with MPA-Texas red streptavidin. Autofluorescence of pulmonary tissue was examined in the sham-treated samples. The images are typical of at least three independent experiments.

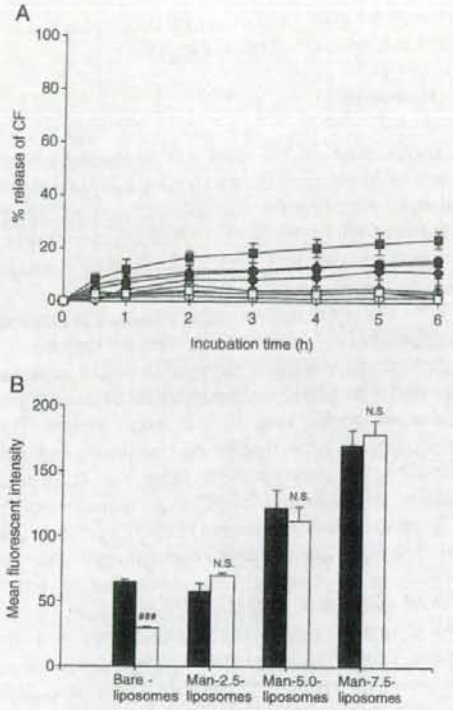

Fig. 8. (A) Effect of pulmonary surfactant on the stability of CF-liposomes. CF-Bare- (◆), CF-Man-2.5- (▲), CF-Man-5.0- (●), and CF-Man-7.5-liposomes (■) were incubated with HBSS (opened symbols) or 0.1 mg/mL native pulmonary surfactant (filled symbols). At the indicated time points, the release of CF was measured as described in Methods. (B) Effect of pulmonary surfactant on the uptake of 50 μM fluorescent-labeled liposomes in isolated alveolar macrophages. Isolated alveolar macrophages were incubated with each type of liposomes alone (filled column) or with 0.1 mg/mL native pulmonary surfactant (opened column). The mean fluorescence of liposomes associated with the cells was measured following a 2 h-incubation at 37 °C. Each value represents the mean ± S.D. of three experiments. Statistically significant differences (###$P<0.001$) compared with a control of each group. N.S., not significant.

3.7. Effect of pulmonary surfactant (PS) on stability and uptake of liposomes

To investigate the effect of the physiological environment in the lung on the stability and uptake of liposomes, the release of CF from CF-liposomes and the uptake in the presence of native PS were studied (Fig. 8A). All CF-liposomes showed a release of CF around 10–20% in the presence of 0.1 mg/mL native PS during a 6 h-incubation, regardless of the content of Man-C4-Chol which was comparable to control. After co-incubation with PS, the uptake of Man-liposomes was not

influenced by PS, while that of Bare-liposomes was significantly inhibited ($P<0.001$) (Fig. 8B).

4. Discussion

The purpose of this study was to assess the targeting efficiency of Man-liposomes to alveolar macrophages. This is the first study reporting the successful delivery of Man-liposomes, in terms of internalization, to alveolar macrophages via intratracheal administration since internalization is a crucial factor affecting the efficiency of delivery systems.

To evaluate the uptake and internalization characteristics of Man-liposomes via the mannose receptor-mediated mechanism in alveolar macrophages, isolated alveolar macrophages were incubated with Man-liposomes with an excess of mannan. The cellular association (Fig. 2) and internalization (Fig. 3A) of Man-liposomes were significantly enhanced and significantly inhibited in the presence of mannan (Fig. 2). In addition, the extensive internalization of Man-liposomes was demonstrated by the *in vitro* confocal images (Fig. 3B) corresponding to the *in vitro* uptake study. These results provide the evidence of the enhanced uptake of Man-liposomes via a mannose receptor-mediated mechanism in alveolar macrophages.

As shown in Figs. 1–3, Man-liposomes with the higher mannose density underwent more extensive uptake in alveolar macrophages compared to liposomes with a lower density. This trend is in agreement with our previous study of the uptake characteristics of mannosylated emulsions by primary cultured peritoneal macrophages [34]. Therefore, the large number of mannose residues on the surface of liposomes could initiate sufficient interaction with mannose receptors leading to the internalization of Man-liposomes in alveolar macrophages.

In vivo targeting of Man-liposomes could not be predicted due to the influence of the physiological environment although Man-liposomes showed substantial internalization in alveolar macrophages *in vitro*. Therefore, the accumulation of Man-liposomes in alveolar cells was determined after intratracheal administration to rats. The *in vivo* study demonstrated the increased uptake of Man-liposomes with lots of mannose residues, mediated by mannose receptors (Fig. 5) concurring with the *in vitro* uptake experiments. In addition, these Man-liposomes were selectively delivered to alveolar macrophages, rather alveolar epithelial type II cells, approximately 15–17 times higher than alveolar epithelial type II cells (Fig. 6). Furthermore, to confirm the pulmonary disposition of Man-liposomes by *in vivo* confocal microscopy, the lung tissue and alveolar epithelial type II cells were stained with specific markers after intratracheal administration of liposomes. The confocal images revealed a high accumulation of Man-liposomes in alveolar macrophages but negligible uptake in alveolar epithelial type II cells (Fig. 7A–B). However, some remaining alveolar macrophages were found after lavage in the alveolar epithelial type II cell stained images (Fig. 7B, upper panel). These results support the view that Man-liposomes are well recognized by mannose receptors leading to efficient targeting to alveolar macrophages with high selectivity after intratracheal administration.

Recently, mannose modified liposomes were suggested to increase uptake in alveolar macrophages [4]. The uptake of mannopyranoside modified liposomes with 1000 nm-size in NR8383, alveolar macrophage cell line and after pulmonary administration in rats were significantly higher than that of non-modified one. Although these results corresponded to our study, particle sizes of these liposomal formulations were substantially different. In previous study by Niven et al. [20] demonstrated the effect of particle size of liposomes on the release of CF after nebulization. The release of CF after nebulization was significantly increased when particle size of liposomes was at least 400 nm and suggested that smaller size liposomes (200 nm) could minimize this effect. Furthermore, the optimal size of liposomes should be dependent upon the type of nebulizer which is used. These results support the view that Man-liposomes in our study which particle sizes were less than 200 nm might be stable during pulmonary administration.

To investigate the influence of the pulmonary environment, especially PS, on the stability of Man-liposomes, the release of CF from CF-liposomes in PS at a physiological concentration [28] was examined. In this study, native PS provokes the release of CF about 10–20% (Fig. 8A) which was 2-times higher than the observations by Abu-Dahab et al. [1] when commercial PS was used at the same surfactant concentration. The discrepancy of these studies could be explained by the difference in source of PS. Bernhard et al. has demonstrated the 2-fold lower concentration of surfactant proteins in commercial surfactant compared with the native one; although the surfactant lipid concentration was similar, that resulted in a reduction in surfactant activity [2]. These results suggest that Man-liposomes are moderately stable in the lung microenvironment.

Surfactant lipids, lipid mixtures in PS, which generally form a lamellar structure and are partly removed by alveolar macrophages, are considered to alter the uptake of Man-liposomes. Therefore, the effect of PS on the *in vitro* uptake of Man-liposomes in alveolar macrophages was investigated. As shown in Fig. 8B, native PS strongly inhibited the uptake of Bare-liposomes but not that of Man-liposomes. These results suggest that the uptake pathway of Man-liposomes is different from that of surfactant lipids which is proposed to be a phospholipid receptor-mediated mechanism in alveolar macrophages [22].

In addition, PS or surfactant-like liposomes, has been used as delivery carrier to alveolar cells [8,29]; however, it seems to be less specific for alveolar macrophages based on the whole lung uptake. After correcting with regard to the total number of cells in the lung [5], the whole lung uptake of surfactant-like liposomes was predominately by alveolar epithelial type II cells, about 2–3 times more than by alveolar macrophages after intratracheal administration in rats [24]. As shown in Fig. 6, we demonstrated that Man-liposomes with a large number of mannose residues exhibited whole lung uptake by alveolar macrophages about 10–17 times higher than that by alveolar epithelial type II cells when corrected with regard to the uptake ratio and total cell number. These observations lead us to believe that Man-liposomes are predominantly taken up by alveolar macrophages after intratracheal administration.

Alveolar macrophage-related respiratory diseases including acute infections and chronic pulmonary diseases are of considerable importance as a cause of serious health problems worldwide resulting in two and three million deaths annually in all age groups [32,33]. Therefore, development of new therapeutic regimens and effective delivery systems to deliver drugs to intracellular sites is needed for the desired pharmacological action in order to prevent deaths from such diseases. Here, we have demonstrated the successful selective targeting into intracellular of alveolar macrophages following intratracheal administration of Man-liposomes in rats. Hence, the information in this study will be valuable for the future use, design, and development of mannosylated liposomes as carriers for such as anti-inflammatory or antimicrobial drugs in the treatment of alveolar macrophage-related refractory diseases.

5. Conclusions

We have demonstrated the efficient targeting to alveolar macrophages of Man-liposomes by increasing the mannose residues expressed on the surface of liposomes. Man-liposomes with a high content of Man-C4-Chol exhibit high affinity for mannose receptors resulting in extensive uptake by alveolar macrophages after intratracheal administration. In addition, Man-liposomes are moderately stable to prevent the release of incorporated drugs in lung microenvironment. These observations suggest that mannosylated liposomes are promising carrier systems for targeting drugs to alveolar macrophages following intratracheal administration.

Acknowledgements

This work was supported in part by Grants-in-Aid for Scientific Research from the Ministry of Education, Culture, Sports, Science, and Technology of Japan, and by Health and Labour Sciences Research Grants for Research on Advanced Medical Technology from the Ministry of Health, Labour and Welfare of Japan.

References

[1] R. Abu-Dahab, U.F. Schäfer, C. Lehr, Lectin-functionalized liposomes for pulmonary drug delivery: effect nebulization on stability and bioadhesion, Eur. J. Pharm. Sci. 14 (2001) 37–46.
[2] W. Bernhard, J. Mottaghian, A. Gebert, G.A. Rau, H. Hardt von der, C.F. Poets, Commercial versus native surfactants: surface activity, molecular components, and the effect of calcium, Am. J. Respir. Crit. Care Med. 162 (2000) 1524–1533.
[3] W.T. Cefalu, Concept, strategies, and feasibility of noninvasive insulin delivery, Diabetes Care 27 (2004) 239–246.
[4] S. Chono, T. Tanino, T. Seki, K. Morimoto, Uptake characteristics of liposomes by rat alveolar macrophages: influence of particle size and surface mannose modification, J. Pharm. Pharmacol. 59 (2007) 75–80.
[5] J.D. Crapo, M. Peters-Golden, J. Marsh-Salin, J.S. Shelburne, Pathologic changes in the lungs of oxygen-adapted rats: a morphometric analysis, Lab. Invest. 39 (1978) 640–653.
[6] C. D'Onofrio, F. Paradisi, D. Piccolo, The influence of some metabolic inhibitors on in vitro phagocytizing macrophages. I. The behaviour of human macrophages, Med. Microbiol. Immunol. (Berl) 163 (1977) 195–207.
[7] S. Gelperina, K. Kisich, M.D. Iseman, L. Heifets, The potential advantages of nanoparticle drug delivery systems in chemotherapy of tuberculosis, Am. J. Respir. Crit. Care Med. 172 (2005) 1487–1490.
[8] J.J. Haitsma, U. Lachmann, B. Lachmann, Exogenous surfactant as a drug delivery agent, Adv. Drug Deliv. Rev. 47 (2001) 197–207.
[9] Y. Hattori, S. Kawakami, K. Nakamura, F. Yamashita, M. Hashida, Efficient gene transfer into macrophages and dendritic cells by in vivo gene delivery with mannosylated lipoplex via the intraperitoneal route, J. Pharmacol. Exp. Ther. 318 (2006) 828–834.
[10] N. Ishimoto, T. Nemoto, K. Nagayoshi, F. Yamashita, M. Hashida, Improved anti-oxidant activity of superoxide dismutase by direct chemical modification, J. Control. Release 111 (2006) 204–211.
[11] S. Kawakami, A. Sato, M. Nishikawa, F. Yamashita, M. Hashida, Mannose receptor-mediated gene transfer into macrophages using novel mannosylated cationic liposomes, Gene Ther. 7 (2000) 292–299.
[12] S. Kawakami, J. Wong, A. Sato, Y. Hattori, F. Yamashita, M. Hashida, Biodistribution characteristics of mannosylated, fucosylated, and galactosylated liposomes in mice, Biochim. Biophys. Acta 1524 (2000) 258–265.
[13] M. Khoury, P. Louis-Plence, V. Escriou, D. Noel, C. Largeau, C. Cantos, D. Scherman, C. Jorgensen, F. Apparailly, Efficient new cationic liposome formulation for systemic delivery of small interfering RNA silencing tumor necrosis factor alpha in experimental arthritis, Arthritis Rheum. 54 (2006) 1867–1877.
[14] B.L. Largent, K.M. Walton, C.A. Hoppe, Y.C. Lee, R.L. Schnaar, Carbohydrate-specific adhesion of alveolar macrophages to mannose-derivatized surfaces, J. Biol. Chem. 259 (1984) 1764–1769.
[15] Y.C. Lee, C.P. Stowell, M.J. Krantz, 2-imino-2-methoxyethyl 1-thioglycosides: new reagents for attaching sugars to proteins, Biochemistry 15 (1976) 3956–3963.
[16] C. Lombry, C. Bosquillon, V. Préat, R. Vanbever, Confocal imaging of rat lungs following intratracheal delivery of dry powders or solutions of fluorescent probes, J. Control. Release 83 (2002) 331–341.
[17] R.J. Mason, S.R. Walker, B.A. Shields, J.E. Henson, M.C. Williams, Identification of rat alveolar type II epithelial cells with a tannic acid and polychrome stain, Am. Rev. Respir. Dis. 131 (1985) 786–788.
[18] M.M. Monick, G.W. Hunninghake, Second messenger pathways in pulmonary host defense, Annu. Rev. Physiol. 65 (2003) 643–667.
[19] N.P. Mullin, K.T. Hall, M.E. Taylor, Characterization of ligand binding to a carbohydrate-recognition domain of the macrophage mannose receptor, J. Biol. Chem. 269 (1994) 28405–28413.
[20] R.W. Niven, M. Speer, H. Schreier, Nebulization of liposomes. II. The effects of size and modeling of solute release profiles, Pharm. Res. 8 (1991) 217–221.
[21] P. Opanasopit, M. Sakai, M. Nishikawa, S. Kawakami, F. Yamashita, M. Hashida, Inhibition of liver metastasis by targeting of immunomodulators using mannosylated liposome carriers, J. Control. Release 80 (2002) 283–294.
[22] D.L. Poelma, M.R. Ju, S.C. Bakker, L.J. Zimmermann, B. Lachmann, J.F. Iwaarden van, A common pathway for the uptake of surfactant lipids by alveolar cells, Am. J. Respir. Cell Mol. Biol. 30 (2004) 751–758.
[23] D.L. Poelma, L.J. Zimmermann, W.A. Cappellen van, J.J. Haitsma, B. Lachmann, J.F. Iwaarden van, Distinct effects of SP-B and SP-C on the uptake of surfactant-like liposomes by alveolar cells in vivo and in vitro, Am. J. Physiol., Lung Cell. Mol. Physiol. 287 (2004) L1056–L1065.
[24] D.L. Poelma, L.J.I. Zimmermann, H.H. Scholten, B. Lachmann, J.F. Iwaarden van, In vivo and in vitro uptake of surfactant lipids by alveolar type II cells and macrophages, Am. J. Physiol., Lung Cell. Mol. Physiol. 283 (2002) L648–L654.
[25] R.H. Simon, J.P. McCoy, A.E. Chu, P.D. Dehart, I.J. Goldstein, Binding of *Griffonia simplicifolia* I lectin to rat pulmonary alveolar macrophages and its use in purifying type II alveolar epithelial cells, Biochim. Biophys. Acta 885 (1986) 34–42.
[26] K. Sou, B. Goins, S. Takeoka, E. Tsuchida, W.T. Phillips, Selective uptake of surface-modified phospholipids vesicles by bone marrow macrophages *in vivo*, Biomaterials 28 (2007) 2655–2666.
[27] B.C. Trapnell, J.A. Whitsett, K. Nakata, Pulmonary alveolar proteinosis, N. Engl. J. Med. 349 (2003) 2527–2539.
[28] M. Tsan, G.L. Tsan, J. White, Surfactant inhibits cationic liposome mediated gene transfer, Hum. Gene Ther. 8 (1997) 817–825.

[29] C. Vermehren, S. Frokjaer, T. Aurstad, J. Hansen, Lung surfactant as a drug delivery system, Int. J. Pharm. 307 (2006) 89–92.
[30] S.P. Vyas, S. Quraishi, S. Gupta, K.S. Jaganathan, Aerosolized liposome-based delivery of amphotericin B to alveolar macrophages, Int. J. Pharm. 296 (2005) 12–25.
[31] T.E. Weaver, J.A. Whitsett, Function and regulation of expression of pulmonary surfactant-associated proteins, Biochem. J. 273 (1991) 249–264.
[32] World Health Organization, Acute Respiratory Infection [Online], The World Health Organization, June 3 2007 http://www.who.int/vaccine_research/diseases/ari/en/index6.html#disease%20burden.
[33] World Health Organization, Chronic Respiratory Diseases [Online], The World Health Organization, June 3 2007 http://www.who.int/respiratory/copd/burden/en/index.html.
[34] W. Yeeprae, S. Kawakami, F. Yamashita, M. Hashida, Effect of mannose density on mannose receptor-mediated cellular uptake of mannosylated O/W emulsions by macrophages, J. Control. Release 114 (2006) 193–201.

Lung Cancer (2007) 57, 187–192

available at www.sciencedirect.com

ScienceDirect

journal homepage: www.elsevier.com/locate/lungcan

LUNG CANCER

Carbohydrate status detecting by PNA is changeable through cancer prognosis from primary to metastatic nodal site: A possible prognostic factor in patient with node-positive lung adenocarcinoma

Yutaka Shio[a,*], Hiroyuki Suzuki[a], Takanori Kawaguchi[b], Jun Ohsugi[a], Mitsunori Higuchi[a], Koichi Fujiu[a], Ryuzo Kanno[a], Akio Ohishi[c], Mitsukazu Gotoh[a]

[a] *First Department of Surgery, Fukushima Medical University, School of Medicine, 1 Hikarigaoka, Fukushima 960-1295, Japan*
[b] *Second Department of Pathology, Fukushima Medical University, School of Medicine, Japan*
[c] *Fukushima Red Cross Hospital, Fukushima, Japan*

Received 19 April 2006; received in revised form 30 January 2007; accepted 7 February 2007

KEYWORDS
Lung adenocarcinoma;
Peanut agglutinin;
Carbohydrates;
Lectin;
Prognosis;
Nodal involvement

Summary Carbohydrates antigens in cancer cells are considered to be important molecules, which may play a critical role for metastasis. To elucidate the prognostic relevance of the expression of peanut agglutinin (PNA) binding carbohydrates in patients with lung adenocarcinoma, we investigated the PNA binding carbohydrates immunohistochemically in both of primary tumors and involving nodal lesions. A total of 62 patients with node-positive primary lung adenocarcinoma, who had undergone complete resection and regional nodes dissection were subjected to this study. There were no significant correlations between PNA staining rates and clinicopathological variables. The survival rate of patients who had positive PNA staining in both of primary tumor and nodal lesion was significantly higher than those of patients in the other groups. Furthermore, the loss of the staining rate of PNA was an independent prognostic factor beside the lymphatic vessel invasion using multivariate analysis. The expression of PNA binding carbohydrates in tumor tissue and nodal lesion would be a novel significant prognostic factor for patients with node-positive lung adenocarcinomas.

1. Introduction

Despite advances in therapeutic modalities, the outcome of patients with lung cancer remains poor. Only about 20% of patients with lung cancer survive for 5 years [1]. Nodal

* Corresponding author. Tel.: +81 24 547 1254; fax: +81 24 548 2735.
E-mail address: salt@fmu.ac.jp (Y. Shio).

0169-5002/$ – see front matter © 2007 Elsevier Ireland Ltd. All rights reserved.
doi:10.1016/j.lungcan.2007.02.007

involvement represents the most critical event responsible for the majority of cancer deaths [2]. Basically, most of the patients with node positive lung cancer have poor prognosis. However, some of the patients have relatively higher survival rate. These data suggest the outcomes of patients with node positive lung cancer are variable. Few studies for the prognostic factor of patients with node-positive lung cancer have been shown [3]. We need certain factor, which can predict the prognosis of patients with node positive lung cancer to avoid the inappropriate treatment.

Cell surface carbohydrates have been shown to possibly play an important role in metastatic processes by influencing cell–cell and cell–substratum interactions [4–6]. Others and we have shown that expression of specific carbohydrate structures correlates with high metastatic potential [3,7,8]. However, the precise types of carbohydrates associated with nodal involvement or prognosis of human lung adenocarcinoma have not been determined. To clarify those questions, we retrospectively evaluated the prognostic value of PNA-binding carbohydrates in patients with node-positive lung adenocarcinoma using the lectin-immunohistchemical staining in metastatic nodes as well as primary tumors.

2. Materials and methods

2.1. Patients

A total of 62 patients of node-positive primary lung adenocarcinoma who had undergone complete resection and regional lymph node dissection at the First Department of Surgery, Fukushima Medical University, School of Medicine, Japan, between 1979 and 1998 were included in the present study. The resected primary tumors were examined macro-

Table 1 Relationship between clinicopathological variables and PNA staining

Clinicopathological variable	*n*	Positive	Loss	(Pos–neg)	(Neg–pos)	(Neg–neg)
Total	62	13	49	8	5	36
Age						
<60	26	6	20	3	0	17
>60	36	7	29	5	5	19
Gender						
Male	31	9	22	2	2	18
Female	31	4	27	6	3	18
Tumor size						
<3 cm	30	6	24	2	3	19
>3 cm	32	7	25	6	2	17
Nodal involvement						
n1	20	6	14	2	1	11
n2,3	42	7	35	6	4	25
p-Stage						
IIA	7	2	5	1	0	4
IIB	10	4	6	0	1	5
IIIA	31	5	26	7	3	16
IIIB	14	2	12	0	1	11
Differentiation						
Well	17	4	3	1	0	2
Mod	35	8	17	6	4	17
Poor	10	1	9	1	1	7
Lymphatic factor						
(−)	15	2	13	2	0	11
(+)	47	11	36	6	5	25
Venous factor						
(−)	32	7	25	2	1	22
(+)	30	6	24	6	4	14
Pleural invasion						
(−)	27	5	22	5	2	15
(+)	35	8	27	3	3	21

Positive: positive staining for PNA in primary lung lesion and in metastatic nodal lesion. Loss: with others, which were included group with PNA-positive primary lesions and PNA-negative nodal lesions (Pos–Neg); those with PNA-negative primary lesions and PNA-positive nodal lesions (Neg–Pos); and those with PNA-negative primary lesions and PNA-negative nodal lesions (Neg–Neg). Data represent number of patients. There was no significant correlation between clinicopathological variables and PNA staining by χ^2 test.

scopically and microscopically to determine the tumor location, tumor size, extent of pleural, lymphatic and venous invasion, and histological type, according to the International Staging System for Lung Tumors. The major clinicopathological characteristics of the patients enrolled in this study are summarized in Table 1. Pleural (p factor), lymphatic (ly factor) and venous (v factor) invasion were determined with elastica Masson staining as well as hematoxylin and eosin staining. Invasion was considered positive or negative based on the presence or absence of cancer cell emboli in the respective vessels after examining all fields of cancerous tissues. All clinicopathological factors were judged by one pathologist based on WHO 1999 [9].

2.2. Technique of lectin immunohistochemistry

Lectin immunohistochemistry was performed according to the methods described previously [10], using biotin-labeled PNA lectin obtained from E.Y. Laboratories (San Mateo, CA). Briefly, 3-mm thick sections were cut from blocks and mounted on glass slides precoated with 0.05% poly-L-lysin solution (Muto Pure Chemicals, Tokyo, Japan). Sections were dewaxed in xylene and dehydrated through graded alcohol solutions. Endogenous peroxidase activity was quenched by a 20 min incubation with 0.3% (v/v) solution of hydrogen peroxide (Wako, Osaka, Japan) in 100% methanol. After incubation with 5% dry skim milk in phosphate-buffered saline for 30 min at room temperature, the sections were incubated overnight at 4 °C with biotin-labeled PNA lectin at a ×200 dilution. Sections for lectin staining were then layered with streptavidin–biotin–peroxidase complex (Nichirei) for 30 min at room temperature. Lectin staining was detected using hydrogen peroxidase/diaminobenzidine. Negative controls were prepared by absorbing lectin activity prior to use with its specific monosaccharide sugar, *N*-acetylgalactosamine, and one known positive section as a control to ensure consistency of staining between batches. Sections were counterstained with Mayer's hematoxylin (Muto Pure Chemicals) before dehydration through graded alcohol solutions and mounting [3].

2.3. Evaluation of lectin immunohistochemical staining

Immunohistochemical staining was examined in at least 1000 cells in random sampling at least 10 high power fields (magnification ×200), and the percentages of positively stained neoplastic cells were estimated. The degree of staining of the carbohydrate epitope was classified as positive or negative according to the percentage of cells showing cytoplasmic staining among the total number of cells (more or less than 50% for lectins) in the primary site [3,11]. In nodal lesions, all cancer cells were counted, and evaluated using the same method as in the primary lesion. Positive PNA stain-

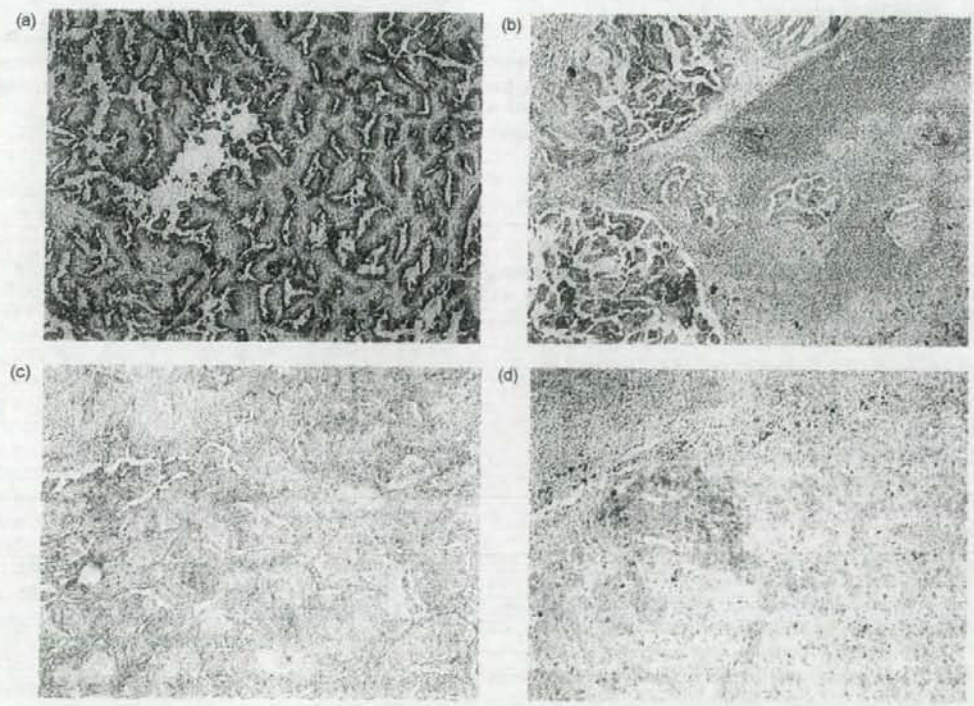

Fig. 1 PNA staining. A case with positive PNA staining: (a) primary lung lesion and (b) metastatic lymph node. A case with lung positive-lymph node negative PNA staining: (c) primary lung lesion and (d) metastatic lymph node (magnification ×100).

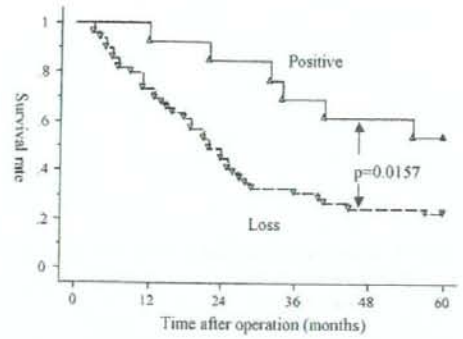

Fig. 2 Survival curves according to PNA staining. Survival curve after surgery. Positive group: PNA-positive primary lesions and PNA-positive nodal lesions. Loss group: with others, which were included group with PNA-positive primary lesions and PNA-negative nodal lesions; those with PNA-negative primary lesions and PNA-positive nodal lesions; and those with PNA-negative primary lesions and PNA-negative nodal lesions. *P* values of log rank test, Cox's model.

ing in the primary lesion is shown in Figs. 1 and 2 (Fig. 1a and b: positive staining of primary lesion and positive nodal lesion, Fig. 1c and d: positive staining of primary lesion and negative nodal lesion).

2.4. Statistical analysis

Data were expressed as mean ± S.D. Differences between groups were examined for statistical significance using the Chi [2] test with Fisher's exact correction. Differences in tumor size and age were examined for statistical significance using the unpaired *t*-test. Cumulative survival rates were calculated by the Kaplan–Meier method and statistical evaluation was performed using the log-rank test. Multivariate analysis was performed using Cox's proportional hazards regression model. The log rank test was used to perform univariate survival analysis. All analyses were performed using StatView 5.0 software (Abacus Concepts, Berkeley, CA). A *P* value less than 0.05 denoted the presence of a statistically significant difference.

3. Results

3.1. Relationship between clinicopathological variables and expression of PNA-binding carbohydrates

Lectin staining rates of PNA in primary lesions and metastatic nodal lesions were 33.9% (21/62) and 29.0% (18/62), respectively. In normal part of the lung of the same sections only a few percent of normal cells were PNA positive and stained weakly. There were no significant correlations between PNA staining rates and clinicopathological variables (age, gender, tumor size, nodal involvement, p-stage, differentiation, lymphatic vessel invasion, blood vessel invasion and pleural invasion) (Table 1).

3.2. Survival analysis

The 5-year survival rate for all patients was 29.0% (stage IIA; 28.6%, IIB; 50%, IIIA; 32.3%, IIIB; 7.0%). The prognosis of patients with poorly differentiated adenocarcinomas was significantly poorer than those with well-differentiated adenocarcinomas. There were no significant correlations between survival and other clinicopathological factors listed in Table 2.

The survival rate according to PNA status of primary lesions was not significant (5-year survival rate: PNA-positive group; 38.1%, PNA-negative group; 24.4%). The survival rate according to PNA status of nodal lesions was also not significant (5-year survival rate: PNA-positive group; 38.9%, PNA-negative group; 25.0%). For further statistical analysis, we divided the 62 patients into two groups: those with PNA-positive primary lesions and PNA-positive nodal lesions (Positive group); and those with others (Loss group), which were included group with PNA-positive primary lesions and PNA-negative nodal lesions; those with PNA-negative primary lesions and PNA-positive nodal lesions; and those with PNA-negative primary lesions and PNA-negative nodal lesions. Kaplan–Meier graph showing the survival in this two group (positive group and loss group) (Fig. 2). The survival rate of patients of the positive group was significantly better than loss group ($p = 0.0157$) (Table 2, Fig. 2).

3.3. Multivariate survival analysis

All data are summarized in Table 3. Staining of PNA and lymphatic vessel invasion were significant independent prognostic factors in the multivariate analysis (odds ratio; 3.680 and 2.794, *P* value; 0.0044 and 0.0185, respectively).

4. Discussion

Our study provides evidence that among patients with pulmonary adenocarcinoma, those with positive expression of PNA-binding carbohydrates in the primary tumor and metastatic lymph nodes have a better prognosis compared with that of other cases, and that negative expression of PNA-binding carbohydrates (negative or loss of expression) either in primary or metastatic lymph nodes may reflect a poor prognosis in this disease. Our study was conducted in order to determine the effect of PNA positivity in primary and metastatic lymph nodes on survival of patients with lung adenocarcinoma. Patients with high PNA expression at the primary site were a heterogeneous group, comprising some who retained and some who lost PNA expression in metastatic lymph nodes. The former had a good prognosis with 5-year survival of 53.8% and the latter group had a poor prognosis with a 5-year survival of 22.4%. The difference between the two groups was highly significant. Patients with negative PNA expression in the primary site, regardless of PNA positivity in metastatic lymph nodes, had a poor prognosis compared to patients with positive PNA expression in both primary and metastatic lymph nodes. Multivariate analysis demonstrated that PNA positivity in primary and metastatic lymph nodes was a highly significant prognostic factor for patients with lymph node metastases of lung adenocarcinoma.

Table 2 Relationship between clinicopathological features and prognosis

Clinicopathological variable	Number	5-year survival (%)	P
Age			
<60	26	30.8	
>60	36	27.7	0.6417
Gender			
Male	31	25.8	
Female	31	32.2	0.6580
Tumor size			
<3 cm	30	33.3	
>3 cm	32	25.0	0.1765
Nodal involvement			
n1	20	35.0	
n2,3	42	26.2	0.4191
p-Stage (II–III)			
II	17	41.2	
III	45	24.4	0.1618
Differentiation (well-others)			
Well	17	47.1	
Others	45	22.2	*0.0266
Lymphatic factor			
(−)	15	46.6	
(+)	47	23.4	***0.0572
Venous factor			
(−)	32	34.4	
(+)	30	23.3	0.1846
Pleural invasion			
(−)	27	33.3	
(+)	35	25.7	0.2261
PNA staining of lung			
Positive	21	38.1	
Negative	41	24.4	0.2611
PNA staining of lymph node			
Positive	18	38.9	
Negative	44	25.0	0.1009
PNA staining of lung and lymph nodes			
Positive	13	53.8	
Loss	49	22.4	*0.0157
Pos–neg	8	12.5	**0.0031
Neg–pos	5	0	**0.0041
Neg–neg	36	27.8	*0.0498

5-Year survival: over all survival rates after operation. Positive: positive staining for PNA in primary lung lesion and in metastatic nodal lesion. Loss: with others, which were included group with PNA-positive primary lesions and PNA-negative nodal lesions (Pos–ng); those with PNA-negative primary lesions and PNA-positive nodal lesions (Neg–pos); and those with PNA-negative primary lesions and PNA-negative nodal lesions (Neg–neg).

* $p < 0.05$.

** $p < 0.01$.

*** $0.05 < p < 0.1$ (p-values of log rank test).

Table 3 Relationship between clinicopathological variables and outcome

Variable	Multivariate analysis		
	Odds ratio	95% CI	P value
n1 vs. n2,3	1.644	0.817–3.311	0.1637
Pleural invasion	1.351	0.713–2.560	0.3563
Lymphatic factor	2.794	1.189–6.566	0.0185
Venous factor	1.108	0.578–2.125	0.7565
Tumor size (>3 cm)	1.098	0.574–2.100	0.7772
Differentiation (well vs. others)	1.952	0.874–4.360	0.1027
PNA (positive vs. loss)	3.680	1.500–9.029	0.0044

Multiple regression, Cox model. CI: confidence interval. Positive: positive staining for PNA in primary lung lesion and in metastatic nodal lesion. Loss: with others, which were included group with PNA-positive primary lesions and PNA-negative nodal lesions (Pos–neg); those with PNA-negative primary lesions and PNA-positive nodal lesions (Neg–pos); and those with PNA-negative primary lesions and PNA-negative nodal lesions (Neg–neg).

PNA is a plant lectin that recognizes βGal/βGalNAc structures including the Thomsen–Friedenreich antigen [12,13]. In normal lung cells, PNA stains the apical surface of type II pneumocytes and Clara cells [14]. Several studies have reported correlations between expression of PNA-binding carbohydrates and clinicopathological factors in various cancers [7,8,15], however, there have been few studies of lung cancer [14,16]. We have previously reported PNA staining rates of 43.3% in lung adenocarcinoma [3]. There has been no report of the relationship between expression of PNA-binding carbohydrates and prognosis and the profiles of distant metastasis of patients with lung cancer. Only a few studies have shown the correlation between the high expression of PNA-binding carbohydrates and the high metastatic ability in the animal model. Our study was novel in its approach of studying the expression of PNA-binding carbohydrates in both primary lesions and metastatic nodal lesions. We report that PNA-binding carbohydrate expression in primary and metastatic nodal lesions is a strong prognostic factor. While the mechanism(s) of PNA-binding carbohydrate expression on prognosis were not determined in the present study, we can speculate on the several possibilities.

Recent studies have demonstrated that modification of carbohydrate properties in cancer cells may alter the cell–cell adhesion capacity [17,18] or immune response to these cells [19]. These changes of carbohydrate properties may therefore regulate the metastatic potential of cancer cells to regional nodes or distant organ [20]. We found in this study that disappearance of PNA-binding carbohydrates in metastatic nodal cancer cells was a marker of poor prognosis. Most of the patients subjected to our study resulted the distant metastasis as the recurrences. Therefore, our results may suggest that loss of PNA binding carbohydrates involve to distant metastasis by the change of ability of cell–cell adhesion or escape from host immune system.

To date many studies, which have shown the correlation between the carbohydrates characteristics and immune

response or adhesion capacities have reported [20–23]. In fact, we have recognized that one of the PNA-binding molecules as decay-accelerating factor, which is one of the complement regulatory molecules, by our recent study (unpublished data).

In summary, loss of PNA-binding carbohydrates may correlates with poor prognosis in patients with node-positive pulmonary adenocarcinoma. Further studies are needed to clarify the detailed role of PNA-binding carbohydrates in the mechanism of metastasis in pulmonary adenocarcinoma. However, we have demonstrated important evidence that a change in PNA-binding carbohydrate structures can affect the survival of patients with lung adenocarcinoma. This novel finding should be of prognostic value in human lung adenocarcinoma.

References

[1] Tsukuma H, Ajiki W, Ioka A, Oshima A, and Research Group of Population-Based Cancer Registry of Japan. Survival of cancer patients diagnosed in 1993–1996: collaborative study of population-based cancer registries in Japan. Jpn J Clin Oncol 2006;36:602–7.

[2] Suzuki H, Kawaguchi T, Sio Y, Fujiu K, Kanno R, Ohishi A, et al. Clinicopathological features of local and metastatic recurrences in primary lung adenocarcinoma. Fukushima J Med Sci 1998;44:13–21.

[3] Suzuki H, Kawaguchi T, Higuchi M, Shio Y, Fujiu K, Kanno R, et al. Expression of peanut agglutinin (PNA lectin) binding carbohydrates correlates with nodal involvement in human lung adenocarcinoma. Cancer Lett 2002;187:215–21.

[4] Nicolson GL. Cell surface molecules and tumor metastasis. Regulation of metastatic phenotypic diversity. Exp Cell Res 1984;150:3–22.

[5] Kawaguchi T. Adhesion molecules and carbohydrates in cancer metastasis. Rinsho Byori 1996;44:1138–46 [in Japanese].

[6] Kannagi R. Carbohydrate-mediated cell adhesion involved in hematogenous metastasis of cancer. Glycoconj J 1997;14:577–84.

[7] Cochran AJ, Wen DR, Berthier-Vergnes O, Bailly C, Dore JF, Berard F, et al. Cytoplasmic accumulation of peanut agglutinin-binding glycoconjugates in the cells of primary melanoma correlates with clinical outcome. Hum Pathol 1999;30:556–61.

[8] Mustac E, Melato M, Sasso F, Valkovic T, Bottin C, Jonjic N. The lectin-binding sites for peanut agglutinin in invasive breast ductal carcinomas and their role as a prognostic factor. J Cancer Res Clin Oncol 1996;122:693–7.

[9] Histological Typing of Lung and Plueral Tumors. International Histological Classification of Tumors. 3rd ed. Geneva: World Health Organization; 1999.

[10] Hsu SM, Raine L, Fanger H. Use of avidin-biotin-peroxidase complex (ABC) in immunoperoxidase techniques: a comparison between ABC and unlabeled antibody (PAP) procedures. J Histochem Cytochem 1981;29:577–80.

[11] Fenlon S, Ellis IO, Bell J, Todd JH, Elston CW, Blamey RW. Helix pomatia and Ulex europeus lectin binding in human breast carcinoma. J Pathol 1987;152:169–76.

[12] Banerjee R, Das K, Ravishankar R, Suguna K, Surolia A, Vijayan M. Conformation, protein–carbohydrate interactions and a novel subunit association in the refined structure of peanut lectin–lactose complex. J Mol Biol 1996;259:281–96.

[13] Ravishankar R, Suguna K, Surolia A, Vijayan M. Structures of the complexes of peanut lectin with methyl-beta-galactose and *N*-acetyllactosamine and a comparative study of carbohydrate binding in Gal/GalNAc-specific legume lectins. Acta Crystallogr D Biol Crystallogr 1999;55:1375–82.

[14] Hachiya T, Honda T, Kubo K, Sekiguchi M. Expression patterns of type II pneumocyte apical surface glycoconjugates in lung adenocarcinoma cells. Virchows Arch 1999;434:63–9.

[15] Howard DR, Ferguson P, Batsakis JG. Carcinoma-associated cytostructural antigenic alterations: detection by lectin binding. Cancer 1981;47:2872–7.

[16] Matsumoto H, Muramatsu H, Muramatsu T, Shimazu H. Carbohydrate profiles shown by a lectin and a monoclonal antibody correlate with metastatic potential and prognosis of human lung carcinomas. Cancer 1992;69:2084–90.

[17] Oda S, Sato M, Toyoshima S, Osawa T. Purification and characterization of a lectin-like molecule specific for galactose/*N*-acetyl-galactosamine from tumoricidal macrophages. J Biochem (Tokyo) 1988;104:600–5.

[18] Zebda N, Bailly M, Brown S, Dore JF, Berthier-Vergnes O. Expression of PNA-binding sites on specific glycoproteins by human melanoma cells is associated with a high metastatic potential. J Cell Biochem 1994;54:161–73.

[19] Ohyama C, Tsuboi S, Fukuda M. Dual roles of sialyl Lewis X oligosaccharides in tumor metastasis and rejection by natural killer cells. EMBO J 1999;18:1516–25.

[20] Cornil I, Kerbel RS, Dennis JW. Tumor cell surface beta 1-4-linked galactose binds to lectin(s) on microvascular endothelial cells and contributes to organ colonization. J Cell Biol 1990;111:773–81.

[21] Fritz P, Seizer-Schmidt R, Murdter TE, Kroemer HK, Aulitzky W, Andre S, et al. Ligands for Viscum album agglutinin and galectin-1 in human lung cancer: is there any prognostic relevance? Acta Histochem 1999;101:239–53.

[22] Engebraaten O, Fodstad O. Site-specific experimental metastasis patterns of two human breast cancer cell lines in nude rats. Int J Cancer 1999;82:219–25.

[23] Fukuda M. Possible roles of tumor-associated carbohydrate antigens. Cancer Res 1996;56:2237–44.

6 臨床試験に入ったミセル体（タキソール内包ミセルNK105）

濱口哲弥（国立がんセンター中央病院消化器内科）

Point

- NK105はタキソールをPEGとP-ASPが鎖状に結合したポリマーによりミセル可溶化した製剤である。1バイアル中にポリマー100mg、タキソール30mgを含有し平均粒径は約90nmである。
- 臨床第Ⅰ試験からは、NK105の推奨投与量である150mg/m^{2}とタキソールの国内承認用量である210mg/m^{2}でCL_{tot}とV_{ss}を比較すると、それぞれ1/25、1/13とNK105のほうが明らかに低く、EPR効果を端的に証明することができた。
- 第Ⅰ相試験より第Ⅱ相試験での推奨投与量は150mg/m^{2}であり、今後、胃がんや卵巣がんなどを対象とした臨床第Ⅱ相試験を計画中であり、速やかな臨床評価が望まれる。
- Abraxaneはアルブミン包埋タキソール粒子で、粒子サイズが約130nmのDDS製剤である。
- 転移性乳がんに対するタキソールとAbraxaneとの第Ⅲ相試験では、grade 3の末梢神経障害はタキソールに比べAbraxaneの方が高頻度にみられたものの、奏効率、無増悪生存期間、grade 3、4の好中球減少はタキソールよりAbraxaneの方が優れた結果が得られた。2005年1月に転移性乳がんに対してFDAの承認が得られ、国内でも治験が行われている。

はじめに

固形がんの治療におけるDDSの役割は、より選択的に薬剤をがん局所に到達させ治療効果を高め、同時に薬物有害反応の軽減を図ることにある。松村らは、生体でのがん組織の特性を検討した結果、一般に固形腫瘍では腫瘍血管の増生と、それに見合うリンパ系システムの増生がなく、また腫瘍血管においては著しい血管透過性の亢進が起きていることを見出し、このことから正常血管では血管外に漏れにくい高分子物質も腫瘍血管からは漏出しやすく、またいったん局所で漏出した高分子はその場に停滞しやすい、いわゆるEPR（enhanced permeability and retention）効果により高分子制がん剤は受動的ターゲティング（passive targeting）が可能となることを明らかにした[1-3]。

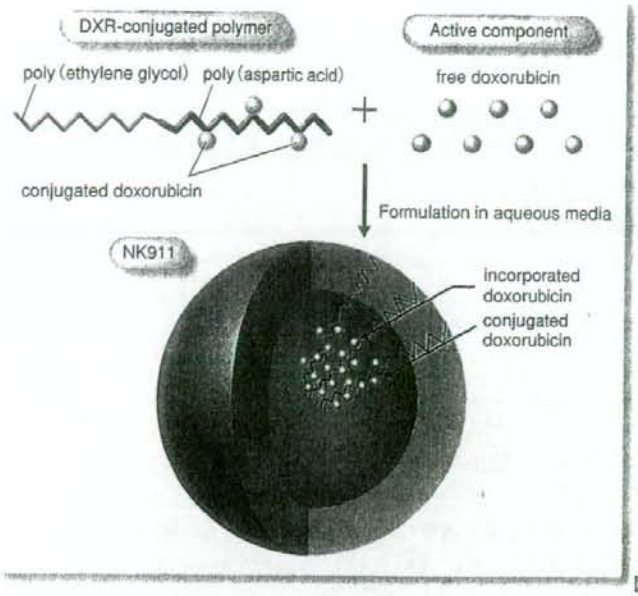

図1 ●ドキソルビシン内包ミセル

粒子径が数10nmで腎糸球体から濾過されない
外殻をPEGで覆うため網内系によるtrapが少ない
長い血中半減期を有する
長期での非蓄積性
高い水溶性
高い薬物安定性
凍結乾燥後も再び容易に水溶液に戻すことができる
外殻の高分子鎖の先端に、目的に応じてパイロット分子を連結できる
疎水性薬剤やペプチドや遺伝子も内包できる

表1 ●DDS製剤としてのミセル体の特徴

高分子ミセルに薬剤を結合させ、その薬剤の徐放に応用しようという案はRingsdorfらにより報告され[4]、その後横山らは、ドキソルビシン（DOX）をミセル内核に封入した高分子ミセルを作成することに成功した[5,6]。このミセルは図1に示すような疎水性ポリマーと親水性ポリマーよりなるAB型ブロックコポリマーの疎水性部分に薬物を導入した薬物-ブロックコポリマー複合体である。高分子ミセルは表1に示すように、薬物の生体内におけるキャリアーとして非常に優れた特徴をもっている。本稿では、国内で臨床第Ⅰ相試験まで開発が進んだタキソールを内包したミセル製剤につき概説する。

タキソール

タキソールは植物アルカロイドで、太平洋イチイの樹皮に由来する抗微小管薬であり、ビンカアルカロイド類とは異なる部位でチューブリンと結合し微小管の脱重合を阻害する。その結果、微小管は細胞周期の必要な時期に解離できず正常な細胞増殖が停止すると考えられている。タキソールは水難溶性であるため、cremophor ELが投与溶媒として使用されており、そのため気管支収縮や蕁麻疹、低血圧などを伴う過敏反応を引き起こすことがあり、このため、ステロイド類や抗ヒスタミン剤を予防投与することが必要となる。しかし、これらの予防投与にもかかわらず1～3%程度で過敏反応が出現するため注意が必要である[7]。また通常の点滴用セットに可塑剤として使用されているDEHP（フタル酸ジエチルヘキシル）を含有しているものは使用できず、特殊な点滴セットを使用しなければならない。

タキソールは卵巣がん、乳がん、非小細胞肺がん、胃がん、子宮体がんに対して適応承認されている。タキソールの毒性は、催吐作用は軽度で好中球減少と末梢神経障害が用量制限毒性（dose-limiting toxicities；DLT）である[8]。好中球減少は0.05～0.1 μMの血中濃度持続時間との相関が報告されており、長時間投与では低濃度の持続時間延長によって好中球減少が高度となるため、通常1～3時間投与が主流である。末梢神経障害は投与継続により発現頻度が高まる蓄積性の毒性である。感覚鈍麻もしくは過敏、ビリビリとしたしびれ感、灼熱感などの知覚異常が四肢遠位端優位に発現する。このような神経障害への対処法は確立していないため、神経障害の程度が強くなると抗腫瘍効果が持続していても治療を休止もしくは中止しなくてはならない厄介な毒性である。

タキソール内包ミセルの前臨床試験[9]

タキソールをミセルに内包化することにより、有機溶媒なしに安全かつ簡便に投与可能となることが期待できる。また高分子化によるEPR効果により薬剤の腫瘍集積性を増すとともに、体内組織（臓器）への薬剤分布を変えることにより、タキソールで実地臨床において問題となっている蓄積性末梢性神経障害の克服につながることを期待し、タキソール内包ミセルの開発が進められた。種々の改良を経て臨床用製剤NK105が作製された。

NK105はタキソールをPEGとP-ASPが鎖状に結合したポリマーによりミセル可溶化した製剤である。1バイアル中にポリマー100mg、タキソール30mgを含有し平均粒径は約90nmである（図2）。培養ヒトがん細胞に対する増殖抑制効果をNK105とタキソールで比較検討したところ、用量反応曲線およびIC50は両者ともほぼ同等であった（表2）。次にヒト大腸がんHT-29に対する抗腫瘍効果を比較検討した。ヌードマウスにヒト大腸がん株HT-29を皮下移植し、腫瘍径が約5mmになった時点でタキソールおよびNK105をタキソール当量100mg/kg、50mg/kg、25mg/kgを週1回、3週にわたり尾静脈より投与した。すべての投与群でNK105の抑制率がタキソールのそれを有意に上回り、タキソールの100mg/kg群とNK105の25mg/kg群とがほぼ同等の抗腫瘍効果を示した。さらにNK105の100mg/kg投与群では全例で腫瘍の消失を認め観察期間中に再発を認めず、タキソール投与では得られない優れた効果を示した。またタキソールの100mg/kgとNK105の100mg/kg投与群とでは後者のほうが体重減少は軽度であった（図3）。次にミセル化により末梢神経毒性が軽減することができるかを検討した。ICRFマウスにタキソールおよびNK105をタキソール当量25mg/kg/日、連続5回静注後、神経病理学的および電気生理学的に比較した。神経病理学的検討では、NK105群ではタ